Third International Symposium on Marine Propulsors
smp'13, Launceston, Tasmania, Australia, May 2013

Flexible Elliptic Oscillating Duct. Taking the FOD one step further.

Gerasimos Politis[1],Theodoros Ioannou[2], Vasileios Tsarsitalidis[3]

[1]Associate professor, NTUA, Athens Greece, polit@central.ntua.gr
[3]Naval Architect and Marine Engineer Senior Student, NTUA Athens, Greece
[3]Naval Architect and Marine Engineer, Ph.D. candidate, NTUA Athens, Greece, vtsars@central.ntua.gr

ABSTRACT

Inspired by the paradigm of a jellyfish or a torpedo fish, we have extended the FOD (Flexible Oscillating Duct) concept to the new FEOD (Flexible Elliptic Oscillating Duct) concept. The FEOD is a generalization of the FOD since it can have an elliptic shape when at rest and can oscillate differently along the two axis of the ellipse. By leaving the major axis of the ellipse constant in time, the FEOD can be supported to the ship's hull, a problem which was very difficult to be solved for a FOD. In this case the oscillation of the FEOD is limited to the minor axis of the ellipse. Apart from the obvious advantage of having two points of support, the FEOD is also capable of better adaptation to the existing area behind the ship, allowing thus lower thrust coefficients, and higher efficiencies. To understand the flow physics of the FEOD system, the problem of flow around an actively (i.e. controlled by the user) deforming FEOD, performing unsteady motion, while travelling with a given velocity in an infinitely extended fluid, has been simulated using the Unsteady Boundary Element Modeling code UBEM. For the needs of the simulation, a special data generation algorithm has been developed, capable of producing a number of unsteady motions for the FEOD, including chord-wise flexibility. Using this data-generation code, we feed UBEM with systematic motion data by varying the pitch angle of the FEOD sections, as well as the Strouhal number. Systematic results for the open water thrust, power and efficiency are calculated and presented. The problem of designing such a system for a real ship is also presented. Comparisons with a conventional propeller and a similar FOD prove that the FEOD is a promising system, more feasible than the FOD, with propulsive efficiencies comparable to that of a conventional propeller.

Keywords

Biomimetic Propulsion; Jellyfish Propulsion; Flexible oscillating Duct; Unsteady wake rollup.

1. INTRODUCTION

In Politis and Tsarsitalidis (2012) the concept of a FOD (Flexible Oscilating Duct) has been introduced as a new propulsor. In the same paper the design methodology of the FOD has been presented and comparisons with a conventional propeller, for three different ship types have been given. The main conclusion from this work was that the FOD is a promissing propulsor with hydrodynamic efficiencies well over that of a convensional propeller. The main disadvantage of the FOD has to do with his support to the hull stern. More specifically it became obvious from the beginning that the completely circular geometry of the FOD makes difficult its support onto the ship, since every single point of the FOD would be in a constant motion. Towards resolution of this problem we decided to expand/generalize the geometry of our propulsor allowing elliptical shapes. We thus arrive to the concept of a 'Flexible Elliptic Oscillating Duct' or simply, FEOD. An important difference between the FOD and the FEOD is that the latter can oscillate in both axis of the ellipse in a manner determined by the designer. This allows the designer to select one of the axis of the ellipse (for example the major axis) to be constant and the other to be oscillating. With this selection the major axis can be used for supporting the FEOD to the hull. Hence both ducts (FOD & FEOD) oscillate, but since the FEOD has two degrees of oscillation freedom (the two axis of the ellipse), deforms as an ellipse rather than as a circle in the general case.

In this paper the FEOD is introduced and systematically examined. Hydrodynamic performance simulations are then undertaken using UBEM, Politis (2004,2011), in a pilot, limited in extent, systematic series for the FEOD and the calculated mean thrust and power are plotted in diagrams, appropriate for the FEOD design. Systematic runs include variation of Strouhal number and pitch angle amplitude for a pre-selected FEOD geometry. A design method, that employs the produced charts, is presented and used to calculate the powering performance of a passenger/car ferry equipped with the FEOD propulsor.

Powering performance calculations have also been made for the same ship equipped with either a FOD or a conventional propeller. The comparison shows that the FEOD can produce high efficiencies, although not as high as the FOD, but good enough to give a serious reason for further investigating such a propulsor and overcoming the technical difficulties connected with its construction.

2. FEOD geometry and motion – panel generation.

The starting point for an unsteady BEM simulation of a flexible body is the generation of the time dependent paneling describing the geometry of the system, Politis (2011). Thus we start from a discussion of the shape of the FEOD with a special consideration on the definition of the 'FEOD sections' and their 'pitch'.

Consider a plane Cartesian orthogonal coordinate system YZ, figure 1. There are three common descriptions for an elliptic shape with major and minor axis A, B as follows:

$$\frac{z^2}{A^2}+\frac{y^2}{B^2}=1 \tag{1}$$

$$z = A\cdot\cos(\tau) \tag{2}$$

$$y = B\cdot\sin(\tau) \tag{3}$$

$$z = r\cdot\cos(\varphi) \tag{4}$$

$$y = r\cdot\sin(\varphi) \tag{5}$$

where r, φ, τ are related by the equations:

$$r = \frac{1}{\sqrt{\frac{\cos^2\varphi}{A^2}+\frac{\sin^2\varphi}{B^2}}} \tag{6}$$

$$\tan\varphi = \frac{B}{A}\tan\tau \tag{7}$$

Equation (1) is the standard form, while equations (2),(3) and equations (4),(5) are parametric forms, with $\tau\in(0,2\pi)$ and $\varphi\in(0,2\pi)$ respectively. Form (2),(3) is termed 'concentric' in the sequel while form (4),(5) is termed 'polar'. The parameter φ in the description of the polar form has a very simple physical meaning. It denotes the angle of the line segment $\overline{OE}$ starting at the center of the ellipse O and ending at the point E belonging to the ellipse, figure 1. In the same figure the physical meaning of the parameter τ is shown.

The YZ system of figure 1, can now be completed to a right handed 3D Cartesian-orthogonal coordinate system, by adding the X-axis normal to YZ showing inside paper. We can now proceed to the description of FEOD by 'building' the FEOD hydrodynamic sections around this ellipse. More specifically the ellipse of figure 1 is selected to be the locus of the pitch axis points of the FEOD sections. To complete the FEOD geometry, the position of the FEOD sections in space has to be defined. Figure 1 dictates two alternatives for this:

(a) *polar case*: put the section in the plane defined by the X-axis and the line $\overline{OE}$ (angle φ from Z-axis), or

(b) *concentric case*: put the sections in a plane through E with orientation parallel to the plane defined by the X-axis and the line $\overline{OE''}$ (angle τ from Z-axis) .

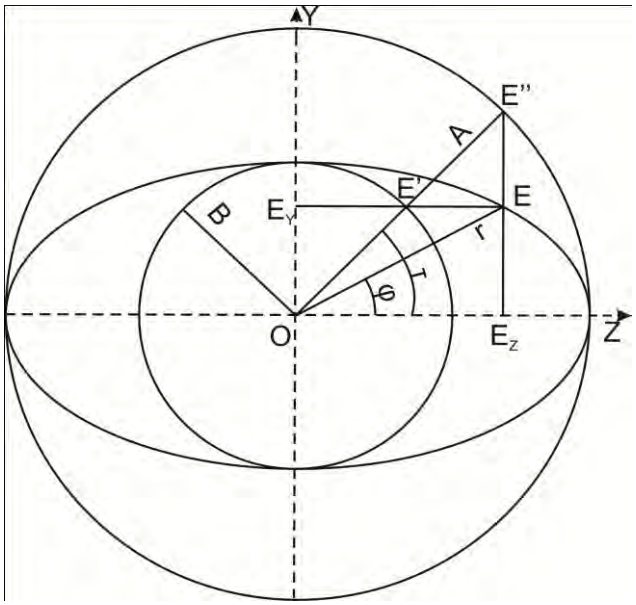

Figure 1. Inscribed and outscribed circles of an ellipse. Points E, E', E_Y define a line parallel to Z-axis, while points E'', E, E_Z define a line parallel to Y-axis

Orientate then the FEOD section, at either plane, to make an angle θ with the X-axis. In general θ can be a function of φ or τ i.e. $\theta(\varphi)$ or $\theta(\tau)$. Assuming further that the following variables are known functions: (i) the FEOD chord distribution $c(\varphi)$ ($c(\tau)$), (ii) the maximum camber distribution $f(\varphi)$ ($f(\tau)$), (iii) the maximum thickness distribution $T(\varphi)$ ($T(\tau)$), (iv) the thickness and camber forms, and (v) the chordwise position b for the sectional pitch axis from leading edge, the geometry of the FEOD is fully defined.

The two alternatives (a) and (b) lead to two different space grids which shall be termed as the 'polar grid' and the 'concentric grid' respectively, in accordance with the previous definitions regarding the parametric description of an ellipse.

We can now add a heaving motion to the pitch loci ellipse of figure 1, as follows. Assume:

$$A = A_0 + A_1\cdot\sin\left(\omega\cdot t+\psi_A\right) \tag{8}$$

$$B = B_0 + B_1\cdot\sin\left(\omega\cdot t+\psi_B\right) \tag{9}$$

where A_0, B_0 denote the mean major and minor axis positions and A_1, B_1 the corresponding oscillation amplitudes, ω denotes the angular velocity of oscillation which is common for both axis ($\omega = 2\pi n$ where n the frequency of oscillation) and ψ_A, ψ_B the phase angles.

With the previous considerations in mind, the points on the ellipse are identifiable through a certain value of the parameter φ (polar description/grid) or the parameter τ (concentric description/grid). Considering now the motion induced by relations (8),(9) to point E, we observe that this depends on the parametric identification used for E i.e. it is different for the concentric and polar descriptions. Dividing the two sides of the polar equations (4),(5) we get:

$$\frac{y}{z} = \tan\varphi \tag{10}$$

Relation (10) indicates that if we use the polar description to parameterize the points of the ellipse, then the $E(\varphi)$ moves along $\overline{OE}$ i.e. in-plane with the FEOD section. Denote by $dr(\varphi,t)/dt$ the 'heaving velocity' on the polar plane (r according to equation (6)). The total sectional undisturbed velocity due to the combined polar plane heaving and parallel translation V can then be calculated: $V^* = \sqrt{V^2 + \left(dr(\varphi,t)/dt\right)^2}$ and the angle $\phi(\varphi,t)$ between velocities V and V^* is given by the relation:

$$\phi(\varphi,t) = \tan^{-1}\left(\frac{dr(\varphi,t)/dt}{V}\right), \tag{11}$$

The sectional pitch angle $\theta(\varphi,t)$ can then be selected according to the formula:

$$\theta(\varphi,t) = w\cdot\phi(\varphi,t) = w\cdot\tan^{-1}\left(\frac{dr(\varphi,t)/dt}{V}\right) \tag{12}$$

where w denotes a weighting factor, independent of time, with values in the range: $0 < w < 1$. We name w '*the pitch control parameter*' after Politis & Politis (2012). An estimation of the angle of attack of the wing with respect to V^* is given by the following relation:

$$\alpha(\varphi,t) = \phi(\varphi,t) - \theta(\varphi,t) = (1-w)\cdot\tan^{-1}\left(\frac{dr(\varphi,t)/dt}{V}\right) \tag{13}$$

In this paper we decide to use the polar description/grid for the FEOD discretization. In addition the major axis of the pitch loci ellipse is held constant in time i.e. $A_1 = 0$. Equation (6) applied for the minor axis (i.e. $\varphi = \pi/2$) becomes:

$$r(\pi/2,t) = B = B_0 + B_1\cdot\sin\left(\omega\cdot t + \psi_B\right) \tag{14}$$

or introducing the substitutions: $B_0 = R, B_1 = h_0, \psi_B = \psi$ and $h(t) = h_0\cdot\sin\left(\omega\cdot t + \psi\right)$:

$$r(\pi/2,t) = R + h(t) = R + h_0\cdot\sin\left(\omega\cdot t + \psi\right) \tag{15}$$

Getting the time derivative of (15) we get:

$$dr(\pi/2,t)/dt = dh(t)/dt = h_0\omega\cos(\omega t + \psi) \tag{16}$$

and relation (13) for $\varphi = \pi/2$ becomes:

$$a(\pi/2,t) = (1-w)\tan^{-1}(\pi\cdot Str\cdot\cos(\omega\cdot t + \psi)) \tag{17}$$

where Str denotes the Strouhal number defined by:

$$Str = \frac{n\cdot h}{V}, h = 2h_0 \tag{18}$$

Assuming given values for $w, B_0, R, h_0, V, \omega, \psi$ the motion of the FEOD is fully determined and equations (4),(5) and (6) can be used for the determination of the time dependent geometry and corresponding grid for the FEOD. In case of chord-wise flexibility the FEOD deforms in a similar manner to that discussed in Politis & Tsarsitalidis (2012).

Having introduced the analytical description of both geometry and motion of our FEOD, we can now proceed to the creation of a surface panel distribution at consecutive time steps describing the FEOD geometric evolution. Figure 2 shows the panel discretization of the FEOD at a number of time instances, corresponding to the maximum, minimum and inflection point positions of a FEOD section in one period. With the FEOD paneling in time known, the code UBEM can be applied to calculate the FEOD unsteady forces, energy requirements and free shear layer evolution.

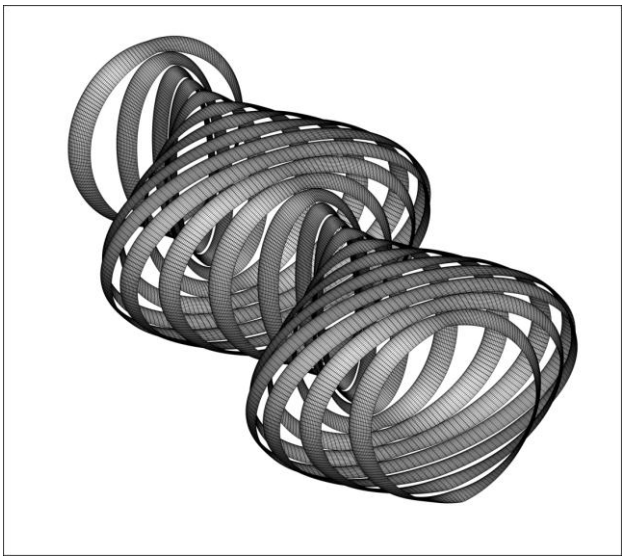

Figure 2. Successive positions of the FEOD in two periods, R/c=B_0/c=4, h_0/c=3, Str=0.46.

3. Calculation of forces, moments, power and efficiency.

In the case of an arbitrary body (rigid or flexible), energy is transferred through flexibility in a point-wise manner. UBEM code uses a specialized procedure for the calculation of the power provided to the tandem wing configuration, termed DHP (Delivered Horse Power) and the useful power developed by the system to propel the ship, termed EHP (Effective Horse Power). The corresponding methodology has already been presented in

Poltis & Tsarsitalidis (2012).

4. Formulation and solution of the FEOD propulsor design problem.

FEOD Propulsor design problem consists in finding the propulsor geometric and motion characteristics by which it can propel a given ship with a given speed. Although the optimum propulsor problem is a problem of mutual propulsor/stern optimization, in most cases we optimize the propulsor assuming that the hull/stern geometry is given.

Development of a design theory for a new propulsor, requires decisions regarding the independent geometric/motion variables controlling the thrust production and the energy absorption. The proposed FEOD propulsor is a generalization of the FOD which has been discussed in detail in Politis & Tsarsitalidis (2012). From paragraph 2 (above), it became obvious that, the FEOD geometry is controlled by two 'length' variables i.e. the sizes of the major and the minor axis, while only the FOD radius characterizes the FOD. Working on the same lines as in Politis & Tsarsitalidis (2012), the non-dimensional variables controlling the FEOD geometry and motion are the following (assuming $\psi = 0$):

$$w, Str, h_0/c, b/c, B_0/c, R/c, \quad \text{camber \& thickness distributions.} \tag{19}$$

A well-posed propulsion problem for a FEOD can be set as follows:

Calculate the instantaneous open water FEOD performance using UBEM for a range of the parameters (w, Str) assuming given $h_0/c, b/c, B_0/c, R/c$ and camber & thickness distributions. Calculate then the period-mean values for thrust and delivered power and denote them by: T and DHP respectively. FEOD performance can then be expressed by the following non-dimensional thrust and (delivered) power coefficients:

$$C_T = \frac{T}{0.5\rho U^2 S} = C_T(w, Str, h_0/c, b/c, B_0/c, R/c) \tag{20}$$

$$C_P = \frac{DHP}{0.5\rho U^3 S} = C_P(w, Str, h_0/c, b/c, B_0/c, R/c) \tag{21}$$

where S denotes the mean FEOD disc surface area $(=\pi \cdot A_0 \cdot B_0)$. In self-propulsion conditions, we assume that a Taylor wake fraction W is defined by:

$$U = V(1-W) \tag{22}$$

where V is the ship speed. Furthermore a relative rotative efficiency η_R is defined by:

$$\eta_R = \frac{DHP}{DHP_B} \tag{23}$$

where DHP_B denotes the (period-mean) power delivered to the FEOD in self-propulsion conditions. Assuming further that a 'thrust equalization method' has been used for the estimation of FEOD-hull interaction coefficients W, t, η_R (where t denotes the thrust deduction factor), the FEOD thrust and power for the first parametric case, in the self-propulsion conditions becomes:

$$T_B = T = 0.5\rho(V(1-W))^2 S \cdot C_T\left(w, \frac{n \cdot 2h_0}{V(1-W)}, h_0/c, b/c, B_0/c, R/c\right) \tag{24}$$

$$DHP_B\eta_R = 0.5\rho(V(1-w))^3 S \cdot C_P\left(w, \frac{n \cdot 2h_0}{V(1-W)}, h_0/c, b/c, B_0/c, R/c\right) \tag{25}$$

For a self-propelled hull, moving with velocity V, the surrounding fluid interacts with the hull developing a resistance force: $R_0(V)/(1-t)$, where $R_0(V)$ denotes the hull towing resistance. A hull can also pull an object with a force F (case of a tug-boat or a trawler). Then the FEOD thrust, under self-propulsion conditions, is given by:

$$T_B = \frac{R_0(V)}{1-t} + F \tag{26}$$

Assuming that $V, w, c, B_0, R, h_0, b, W, t, \eta_R$ are known parameters, Equations (24),(25),(26) become a non-linear system of three equations with three unknowns: (T, DHP_B, n). This system can be solved for a range of ship speeds: $V \in (V_1, V_2)$ and $w \in [0,1]$. We thus obtain the totality of design solutions for the given ship:

$$DHP_B, n \leftarrow V, w\big|_{given:\ \text{ship},\ c, B_0, R, h_0, b, W, t, \eta_R} \tag{27}$$

The content of Equation (27) can be represented in a 2-D $DHP-n$ diagram in the form of parametric curves of constant V and constant w. Notice that this presentation is similar to that used in conventional propellers, where the propeller pitch ratio P/D is taking the place of w. Using this representation, we can finally extract the required optimum FEOD by selecting the characteristics (geometric and motion) which require the minimum DHP for the given ship speed V.

5. Decisions regarding Geometric and Flow/motion variables for the proposed twin wing series.

To proceed to a series based design process for a FEOD, decisions have to be taken, on the corresponding geometric and flow related parameters. For the needs of the current pilot paper on the subject, the series is limited in extent and consist of only one FEOD system, with $R/c = B_0/c = 4$, $h_0/c = 3.0$ and $b/c = 0.33$. The Strouhal number has been selected in the range:

$Str = 0.1 \div 0.7$. Using our previous experience, this selection is expected to contain the region of maximum hydrodynamic efficiency. Finally the range of the pitch control parameter w has been selected between 0 and 1 which means a corresponding pitch angle $\theta(\varphi,t)$ which includes the full range of thrust producing motions for the various Strouhal numbers.

6. Transient FEOD performance and selection of simulation period.

The main difference between a traditional propeller and a biomimetic propulsor is that the latter produces a period mean thrust as a result of a highly unsteady instantaneous thrust. The simulation method in hand can predict this time dependent thrust but, since it is a time stepping method, initial conditions on motion have to be imposed. A burst starting FEOD is used as the starting condition. In this case a transient phenomenon occurs. Thus the mean period values for thrust or power have to be calculated after the passage of this initial transient phenomenon. To take care for this, time domain simulations have been performed for three periods and for several cases. Indicatively, Figures 3, 4 present the unsteady thrust for two cases.

From these figures it can be concluded that, for the representative selected parameters, the transient phenomenon is limited to the few initial time steps after the burst start. Thus it is safe to use the 2nd period of simulation, to calculate the mean thrust and power to be used in the design charts.

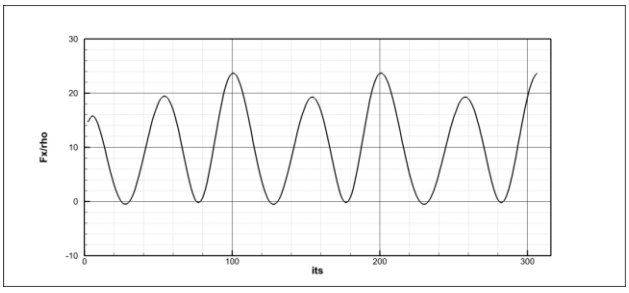

Figure 3. Time evolution of thrust for ($R/c=B_0/c=4$, $h_0/c=3$, Str=0.22, Theta=13.3)

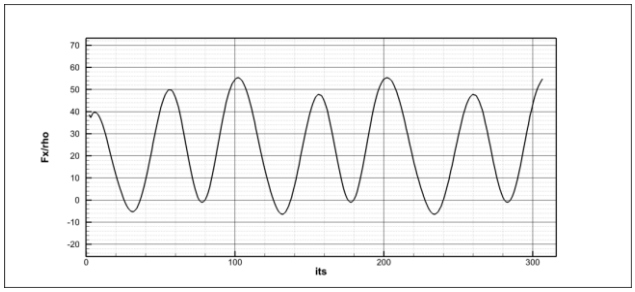

Figure 4. Time evolution of thrust for ($R/c=B_0/c=4$, $h_0/c=3$, Str=0.46, Theta=34.4)

7. Open water performance diagrams and comparison with single wing systems.

Systematic simulations using UBEM have been performed with the selected FEOD series described in section 5. In all simulations a chord of $c = 1.0m$ has been selected. Furthermore in all simulations we have used a FEOD system with: $R/c=B_0/c==4$, $h_0/c=3$,$b/c=0.33$.

Variation of Strouhal number has been achieved by changing the frequency of oscillation while the corresponding translational velocity has been held constant and equal to $V = 2.3m/s$. This results to a constant Reynolds number equal to $0.202 \cdot 10^7$, based on translational velocity ($\mathrm{Re} = V \cdot c / \nu$). Corresponding Reynolds numbers based on the maximum undisturbed flow velocity are Strouhal dependent, according to the relation: $\mathrm{Re}_{Str} = \frac{V \cdot c}{\nu}\sqrt{1+(\pi \cdot Str)^2}$. Thus $\mathrm{Re}_{Str} = 0.22 \cdot 10^7$ at $Str = 0.10$ and $\mathrm{Re}_{Str} = 0.51 \cdot 10^7$ at $Str = 0.7$ (kinematic viscosity: $\nu = 1.139 \cdot 10^{-6} m^2/s$). Mean thrust and power have then been calculated by running the UBEM code for two time periods and calculating the mean values of the unsteady forces over the second period. The results are presented in the form of $C_T - \theta_0$ diagrams, figure 5, (where $\theta_0 \rightarrow theta$ in diagrams) and $C_P - \theta_0$ diagrams, figure 6. Notice that the used θ_0 denotes the sectional pitch angle amplitude along the minor axis of the ellipse (equation (12) with $\varphi = \pi/2$). Notice also that for the FEOD the pitch angle is φ dependent.

$C_T - \theta_0$ diagrams contain additionally in parametric form the open water efficiency η of the system (thin lines):

$$\eta = \frac{T \cdot U}{DHP} = \frac{C_T}{C_P} \tag{28}$$

Also, $C_P - \theta_0$ diagrams contain additionally in parametric form the $a_{\max}$ angle (thin lines) defined as the maximum value of $a(t)$, relation (17) with $\varphi = \pi/2$, over one period. This last information is very useful for the designer in order to avoid maximum angles with a potential danger for separating flow (e.g. greater than 20deg), phenomenon which is not modeled by the used version of UBEM. For illustrative reasons, diagrams 7 and 8 contain similar results for a FOD with : $R/c=4$, $h_0/c=2$, so that comparisons are made easy. Note that the h_0/c ratio is not the same for the two cases, as the h_0/c ratio for the FEOD, refers to the maximum heave at the minor ellipse axis.

Interesting conclusions drawn from those figures are the following: (a) The region of maximum hydrodynamic efficiency is achieved at a maximum angle of attack less than 15degrees i.e. at the region of flow without expected separation, (b) The performance of the FEOD is diminished compared to that of the FOD, but it remains to

be seen if such a compromise is acceptable for the sake of easier construction and proper fixing of the mechanism behind the boat. It should be also noted that systematic inspections of the calculated pressure distributions gave no indication of local pressure less than the corresponding vapor pressure in the region around optimum performance. As a result no cavitation is expected at that region. Finally notice that these charts can be used to select an optimum FEOD configuration for a given ship very easily as discussed in Politis & Tsarsitalidis (2012).

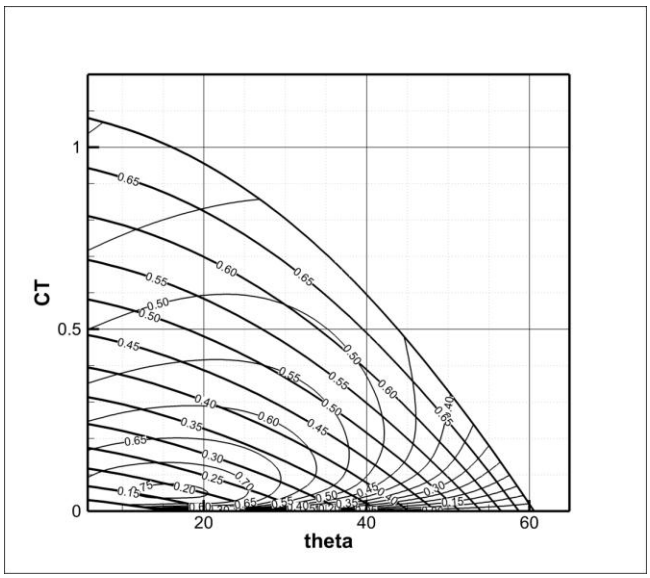

Figure 5. $C_T - \theta_0$ chart for FEOD. Thick lines stand for *Str* and thin lines for Efficiency.

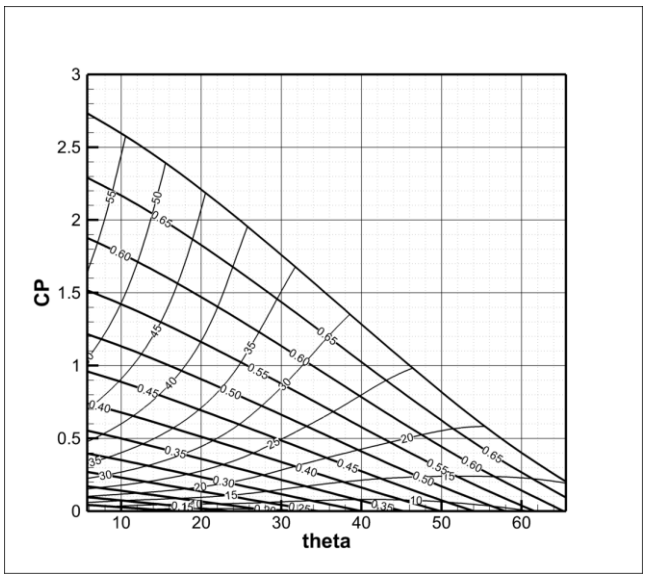

Figure 6 $C_P - \theta_0$ chart for FEOD. Thick lines stand for *Str* and thin for $a_{\max}$

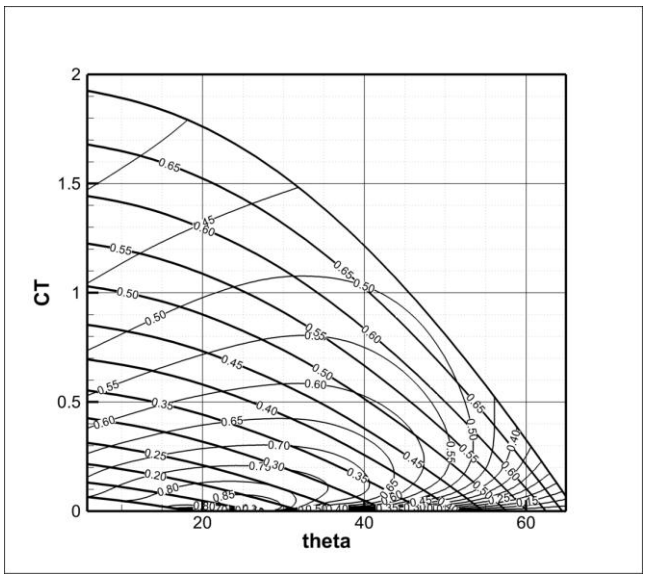

Figure 7 $C_T - \theta_0$ chart for FOD R/c=4 h_0/c=2.0. Thick lines stand for *Str* and thin lines for Efficiency.

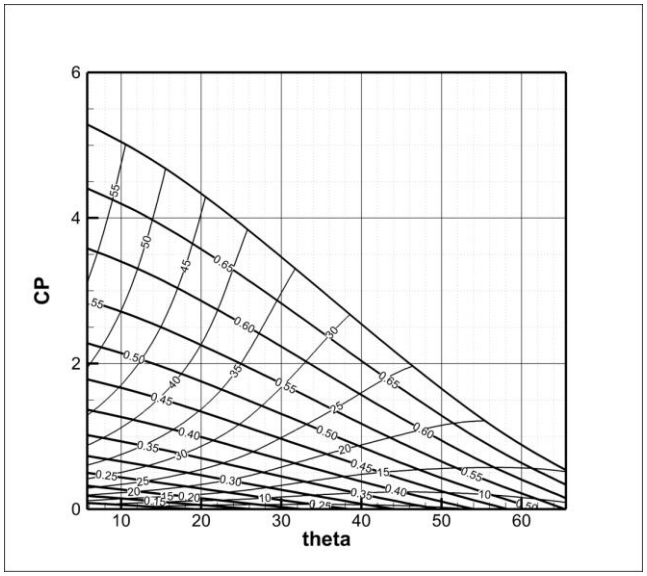

Figure 8 $C_P - \theta_0$ chart for FOD R/c=4 h_0/c=2.0. Thick lines stand for *Str* and thin for $a_{\max}$

8. Wake visualizations – Understanding how the FEOD produces thrust.

For a better understanding of the underlying physical mechanisms of thrust production, the free shear layer produced by the FEOD system is plotted, figures 9a,b. The FEOD surface and the free vortex sheet surface on those figures have been colored according to their surface dipole distribution intensity. Notice that constant dipole lines coincide with surface vortex lines. By using either the last property or the deformation patterns of the free vortex sheets, a number of strong ring vortices in the wake of the FEOD are made recognizable. Those ring vortices produce series of oblique jet flows by which the flapping wing produces thrust. Figure 9 also contains artistic add-

ons, showing the train of ring vortices (toroidal meshes) and corresponding jets (straight arrows) by which the flapping wing feeds with momentum the wake and produces thrust. More specifically the straight arrows are the results of the induced velocities produced by the ring vortices. What is important, is that the wake resembles more that of a twin wing system than that of the FOD (i.e. the homocentric rings have been replaced with couples of rings). From the shape of the rings, it is also noticeable that they resemble the rings produced by wings of small Aspect Ratio operating at lower Strouhal numbers (the rings are elongated in the axis of parallel translation, while in higher AR, they are elongated in the spanwise direction) This fact points to where further investigation is to be made (i.e. higher B_0/c ratios).

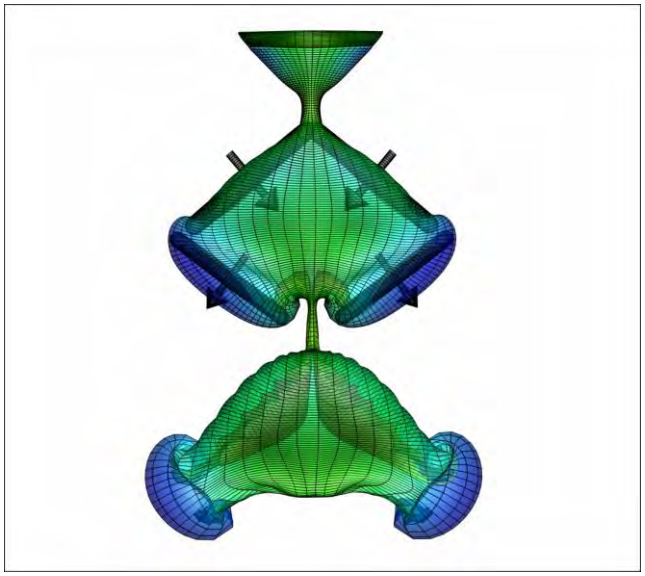

(a)

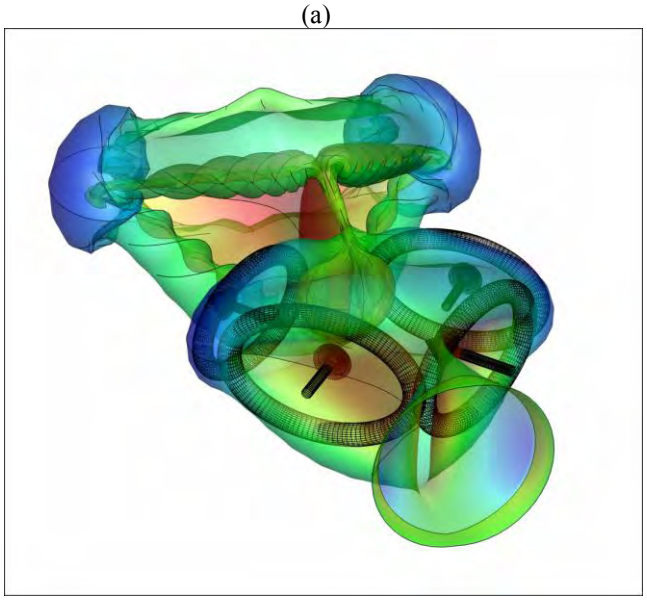

(b)

Figure 9. Wake of a FEOD, Str=0.46, θ_0=34.4. Colors are for dipole potential. Artistic add-ons showing the train of ring vortices and corresponding jets by which the FEOD produces thrust.

9. Application of a FEOD for the propulsion of a ship – Optimum design example.

A passenger ferry is used in a feasibility study for the application of the FEOD, the FOD and a traditional propeller as alternative propulsors, by applying the method explained in Politis & Tsarsitalidis (2012), as expanded in section 4. The passenger ferry is a twin screw vessel with displacement of 8917.66 tons and a maximum allowed propeller diameter of 4.1 meters. The bare hull resistance curve of the ship, taken from the database of the NTUA towing tank, is given in table 1.

With the bare hull resistance given, the system of algebraic equations (24),(25),(26) can be solved for a range of ship speeds V and θ_0, and the totality of design solutions can be presented in a diagram as dictated by Equation (27). For the need of the comparison, it has been assumed that in all cases: $W=0.0, t=0.0, \eta_R=1.0$. This is a reasonable assumption for a twin screw vessel which has small propulsor-hull interactions. The use of the same hull-interaction coefficients for the FEOD/FOD systems and the propeller can be considered reasonable, since interaction coefficients are (for the same stern geometry) mainly functions of propulsor diameter and the developed thrust, Harvald (1983). No inclined axis corrections were made for the conventional propellers. No correction of the bare hull resistance for appendages has been made. A shaft efficiency equal to 1 has been used in the calculations. No corrections for full scale Reynolds number have been introduced for the propulsors.

Totality of design solutions in the form of Constant-V, constant-θ_0 grids for FEOD, FOD and Constant-V, constant-P/D grids for propellers are illustrated for comparison in figures 10,11 and 12. The comparison of the optimum FEOD and FOD vs the optimum B-screw, for a ship speed equal to 23knots can be summarized in table 2. In all cases, the ship is equipped with two propulsors.

Table 1. Resistance curve.

V (m/s)	R(kp)
7.71	31056
8.23	34528
8.75	38374
9.26	42755
9.78	47292
10.29	52301
10.80	58153
11.31	66426
11.83	78009

Table 2. Comparison of propulsors.

Case	Revolutions (rpm)	Power (PS)	Propulsive Efficiency (%)	Power Gain (%)
FEOD	9.81	16211.83	76	5.21
FOD	29.55	14961.13	82	12.52
B-screw	168.30	17103.40	72	

Note, that while the propeller and the FOD, use the maximum allowed (by tolerances) diameter, the FEOD, as it does not move at the upper and lower point, it uses a larger diameter, which in this case, is the maximum diameter the FOD will take (i.e. $D+2h_0$), thus the required Thrust coefficient is lower and the diminished performance of the FEOD is compensated.

It is observed that a gain in propulsive efficiency of 5.21% is obtained for the case of a FEOD in comparison to a conventional propeller. The corresponding gain for a FOD is 12.52%. It is also noticeable, that the optimum flapping wing revolutions are always lower compared to that of corresponding conventional optimum propeller. It should be stretched that the absolute values of power and overall efficiency, contained in table 2, are approximate to the extent of our uncertainty regarding values of propulsor-hull interaction factors.

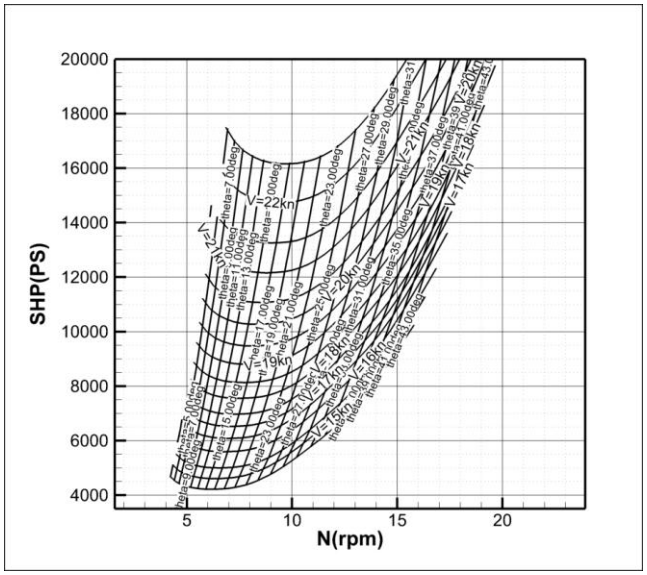

Figure 10. Passenger Ferry-FEOD: Totality of design solutions in the form of Constant-V, constant-θ_0 grid.

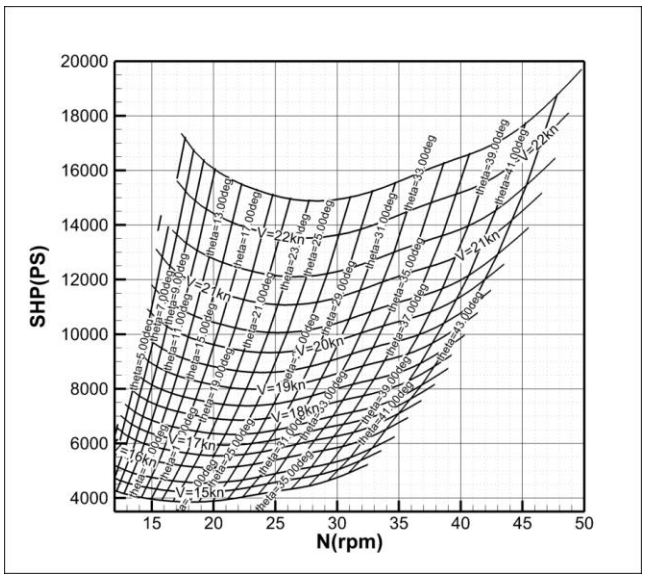

Figure 11. Passenger Ferry-FOD: Totality of design solutions in the form of Constant-V, constant-θ_0 grid.

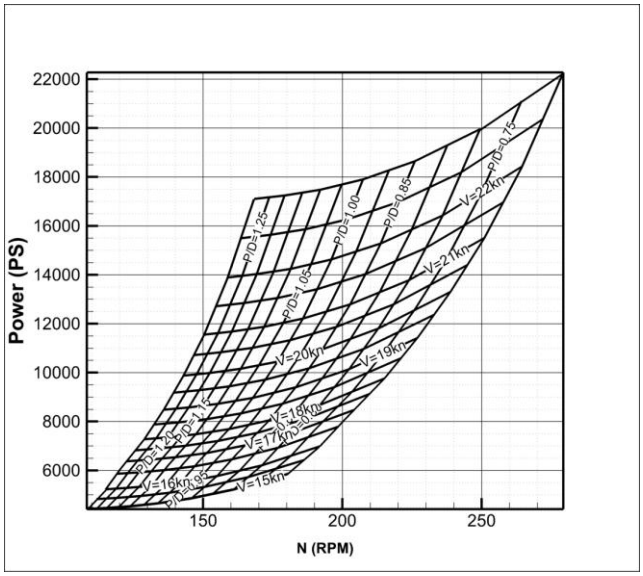

Figure 12. Passenger Ferry- B4.75 screw: Totality of design solutions in the form of Constant-V, constant-P/D grid.

10. Closing remarks, Challenges and further Development

The unsteady boundary element modeling code UBEM has been applied to investigate the open water performance of a FEOD propulsor. Systematic calculations were made and design charts were produced, along with a design methodology, which has been explained thoroughly. Propulsive coefficients of the order of 0.75 have been calculated, which are higher than that observed in conventional propellers. After applying the design method to an actual ship, the FEOD system proves to be better than conventional propellers with respectable efficiency gains of practical interest. The oval shaped swept area and the two fixed points, allow taking

advantage of larger stern area, compared to a propeller, and make it easier to construct and operate, compared to the FOD, which seems feasible only by employing specialized materials. This initial study shows that the loss due to breaking the circular symmetry of the FOD is not big enough to make the system unworthy of further exploration.

Expansion of the presented series of the FEOD, is planned in the near future, a fact which will allow us to examine in more detail the effect of the kinematic and geometric parameters of the propulsor to its hydrodynamic performance.

11. Acknowledgements:

This research has been co-financed by the European Union (European Social Fund – ESF) and Greek national funds through the Operational Program "Education and Lifelong Learning" of the National Strategic Reference Framework (NSRF) - Research Funding Program: Heracleitus II. Investing in knowledge society through the European Social Fund.

REFERENCES

Politis, G. K. (2004). "Simulation of unsteady motion of a propeller in a fluid including free wake modeling." Engineering Analysis with Boundary Elements **28**(6): 633-653.

Politis, G., Politis, K., 'Biomimetic propulsion under random heaving conditions, using active pitch control', Journal of fluids and structures, 2012.

Politis, G. and V. Tsarsitalidis (2012). "Flexible Oscillating Duct: An approach to a novel propulsor." Applied Ocean Research **36**: 36-50.

Politis, G. K. (2011). "Application of a BEM time stepping algorithm in understanding complex unsteady propulsion hydrodynamic phenomena." Ocean Engineering **38**(4): 699-711.